Available online at www.sciencedirect.com
SCIENCE DIRECT®
Journal of Sound and Vibration 291 (2006) 1041–1060
JOURNAL OF SOUND AND VIBRATION
www.elsevier.com/locate/jsvi

Analytical approach to free and forced vibrations of axially loaded cracked Timoshenko beams

C. Mei[a,*], Y. Karpenko[b], S. Moody[b], D. Allen[b]

[a]*Department of Mechanical Engineering, The University of Michigan—Dearborn, 4901 Evergreen Road, Dearborn, MI 48128, USA*
[b]*Brake NVH, Ford Motor Company, 14661 Rotunda Drive, Dearborn, MI 48120, USA*

Received 20 September 2004; received in revised form 8 April 2005; accepted 7 July 2005
Available online 6 September 2005

Abstract

Wave vibration analysis of an axially loaded cracked Timoshenko beam is presented in this paper. It includes the effects of axial loading, shear deformation and rotary inertia. From wave standpoint, vibrations propagate, reflect and transmit in a structure. The transmission and reflection matrices for various discontinuities on an axially loaded Timoshenko beam are derived. Such discontinuities include cracks, boundaries and changes in section. The matrix relations between the injected waves and externally applied forces and moments are also derived. These matrices are combined to provide a concise and systematic approach to both free and forced vibration analyses of complex axially loaded Timoshenko beams with discontinuities such as cracks and sectional changes. The systematic approach is illustrated using several numerical examples.

1. Introduction

The dynamics of cracked structural members, especially beams, has been the subject of many research works mainly due to the growing interests in non-destructive damage evaluation of engineering structures using modal responses (natural frequencies and modeshapes) of a structure in the past two decades. The presence of a crack in a structural member introduces a local

*Corresponding author. Tel.: +1 313 593 5369; fax: +1 313 593 3851.
E-mail address: cmei@umich.edu (C. Mei).

0022-460X/$ - see front matter © 2005 Elsevier Ltd. All rights reserved.
doi:10.1016/j.jsv.2005.07.017

flexibility that affects its dynamic response. Numerous attempts to quantify local defects are reported to the literature. In general, there exist three basic crack models, namely the equivalent reduced section model, the local flexibility model from fracture mechanics and the continuous crack flexibility model [1].

Various approaches have been applied in vibration analysis, mostly free vibration analysis, of cracked beams. Such approaches include finite element approach [2–4], Galerkin and local Ritz approach [5], approximate analytical approach [6], transfer matrix approach [7] and dynamic stiffness matrix approach [8].

In this paper, both free and forced vibrations are studied for an axially loaded cracked Timoshenko beam from wave standpoint, in which the vibrations are described in terms of wave propagation, transmission and reflection in waveguides [9–11]. The reflection and transmission characteristics of flexural vibration waves have been studied by a number of researchers [12–15]. In this study, the transmission and reflection matrices for various discontinuities on an axially loaded cracked Timoshenko beam are derived. Such discontinuities include cracks, boundaries and change in sections. The matrix relations between the injected waves and externally applied forces and moments are also derived. These matrices can be combined to provide a concise and systematic approach to both free and forced vibration analyses of axially loaded cracked Timoshenko beams or complex structures consisting of such beam components. The effects of cracks (including crack size and crack location), axial loads and step sectional changes on the modes of vibrations are studied.

This paper is organized as follows. In the next section, the equation of motion for axially loaded Timoshenko beams is presented and expressions for the propagation of waves derived. In Section 3, the reflection and transmission matrices at discontinuities caused by cracks, boundaries and change in sections are derived. In Section 4, the vectors of wave amplitudes for waves generated by externally applied point forces and moments in a Timoshenko beam are derived. In Section 5, these matrices are combined to provide a concise and systematic approach for vibration analysis of cracked Timoshenko beams or structures consisting of Timoshenko beam components. The approach is illustrated through several numerical examples, including free and forced vibration analyses of a cracked uniform and a cracked stepped Timoshenko beam with axial loading. Concluding remarks are given in Section 6.

2. Equation of motion and wave propagation

The equations of motion of an axially loaded beam with the effects of both shear deformation and rotary inertia taken into account are [9]

$$GA\kappa\left[\frac{\partial\psi(x,t)}{\partial x}-\frac{\partial^2 y(x,t)}{\partial x^2}\right]+F\frac{\partial^2 y}{\partial x^2}+\rho A\frac{\partial^2 y(x,t)}{\partial t^2}=q(x,t) \tag{1a}$$

$$EI\frac{\partial^2\psi(x,t)}{\partial x^2}+GA\kappa\left[\frac{\partial y(x,t)}{\partial x}-\psi(x,t)\right]-\rho I\frac{\partial^2\psi(x,t)}{\partial t^2}=0 \tag{1b}$$

where x is the position along the beam axis, t is the time, $y(x,t)$ is the transverse deflection of the center line of the beam, $q(x,t)$ is the external force, E, G and ρ are the Young's modulus, shear

modulus and mass density, respectively. I is the area moment of inertia of cross section, A is the cross-sectional area, κ is the shear coefficient, $\psi(x,t)$ is the slope due to bending, $\partial y(x,t)/\partial x$ is the slope of the center line of the beam, while $\partial y(x,t)/\partial x - \psi(x,t)$ is the shear angle. F is the axial load, compressive load is assumed positive. It can be seen that Eqs. (1a) and (1b) are coupled through the slope and the transverse deflection of the structure.

The shear force $V(x,t)$ and bending moment $M(x,t)$ at any section of the beam are related to the transverse deflection $y(x,t)$ and the slope $\psi(x,t)$ by

$$V(x,t) = -EI\frac{\partial^2\psi(x,t)}{\partial x^2} - \rho I\omega^2\psi(x,t) - F\frac{\partial y(x,t)}{\partial x}, \tag{2}$$

$$M(x,t) = -EI\frac{\partial\psi(x,t)}{\partial x}. \tag{3}$$

The coefficients

$$C_b = \sqrt{\frac{EI}{\rho A}},\ C_s = \sqrt{\frac{GA\kappa}{\rho A}},\ C_r = \sqrt{\frac{\rho I}{\rho A}}, \tag{4}$$

which are related to the bending stiffness, shear stiffness and rotational effects, respectively, are now introduced. The shear beam model, the Rayleigh beam model and the simple Euler–Bernoulli beam model can be obtained from the Timoshenko beam model by setting C_r to zero (that is, ignoring the rotational effect), C_s to infinity (ignoring the shear effect) and setting both C_r to zero and C_s to infinity, respectively.

2.1. Free wave propagation

Assuming time harmonic motion and using separation of variables, the solutions to Eqs. (1a) and (1b) can be written in the form $y(x,t) = y_0 e^{-ikx}e^{i\omega t}$ and $\psi(x,t) = \psi_0 e^{-ikx}e^{i\omega t}$, where ω is the frequency and k the wavenumber. Substituting these expressions into Eqs. (1a) and (1b) and rewriting the corresponding free vibrations in matrix form, one has

$$\begin{bmatrix} -ikGA\kappa & -EIk^2 - GA\kappa + \rho I\omega^2 \\ -k^2GA\kappa + \rho A\omega^2 + Fk^2 & ikGA\kappa \end{bmatrix}\begin{bmatrix} y_0 \\ \psi_0 \end{bmatrix} = 0. \tag{5}$$

Setting the determinant of Eq. (5) to zero gives a second-order polynomial in k^2—the dispersion equation:

$$a_0k^4 + b_0k^2 + c_0 = 0. \tag{6}$$

The solution to the dispersion equation gives a set of wavenumbers that are functions of the frequency ω as well as the properties of the structure, namely

$$k_1 = \pm\sqrt{\frac{-b_0 + \sqrt{b_0^2 - 4a_0c_0}}{2a_0}},\ \ k_2 = \pm\sqrt{\frac{-b_0 - \sqrt{b_0^2 - 4a_0c_0}}{2a_0}},$$

where

$$a_0 = 1 - \frac{F}{GA\kappa}, \quad b_0 = -k_{b1}^2 - k_{b2}^2 - F\frac{GA\kappa - \rho I\omega^2}{GA\kappa EI}, \quad c_0 = k_{b1}^2 k_{b2}^2,$$

and k_{b1} and k_{b2} are the wavenumbers of the beam without axial loading, that are given by

$$k_{b1} = \pm\left\{\frac{1}{2}\left[\left(\frac{1}{C_s}\right)^2 + \left(\frac{C_r}{C_b}\right)^2\right]\omega^2 + \sqrt{\frac{\omega^2}{C_b^2} + \frac{1}{4}\left[\left(\frac{1}{C_s}\right)^2 - \left(\frac{C_r}{C_b}\right)^2\right]^2\omega^4}\right\}^{1/2},$$

$$k_{b2} = \pm\left\{\frac{1}{2}\left[\left(\frac{1}{C_s}\right)^2 + \left(\frac{C_r}{C_b}\right)^2\right]\omega^2 - \sqrt{\frac{\omega^2}{C_b^2} + \frac{1}{4}\left[\left(\frac{1}{C_s}\right)^2 - \left(\frac{C_r}{C_b}\right)^2\right]^2\omega^4}\right\}^{1/2}.$$

Waves in the beam travel in both the positive and negative directions, as the $\pm$ sign outside the brackets indicates. It is well known that for flexurally vibrating Timoshenko beam without axial loading, there exists a wave-mode transition at a cut-off frequency ω_c, which is given by $\omega_c = C_s/C_r$. The axial loading is found to have no effect on the cut-off frequency. This finding is confirmed by solving the cut-off frequency ω_c directly by substituting $k = 0$ into Eq. (5) and setting the determinant to zero, which gives the same cut-off frequency as that of flexurally vibrating Timoshenko beam without axial loading.

With the time dependence $e^{i\omega t}$ suppressed, the solution to Eq. (5) can be written as

$$y(x) = a_1^+ e^{-ik_1 x} + a_2^+ e^{-k_2 x} + a_1^- e^{ik_1 x} + a_2^- e^{k_2 x}, \tag{7a}$$

$$\psi(x) = \overline{a_1^+} e^{-ik_1 x} + \overline{a_2^+} e^{-k_2 x} + \overline{a_1^-} e^{ik_1 x} + \overline{a_2^-} e^{k_2 x}, \tag{7b}$$

Clearly, the wave amplitudes a of $y(x)$ and $\overline{a}$ of $\psi(x)$ are related to each other. The relation can be found from Eq. (5) as

$$\frac{\psi}{y} = i\frac{\rho A\omega^2 - k^2 GA\kappa + Fk^2}{kGA\kappa}. \tag{8}$$

Thus, the relations between the coefficients of $y(x)$ and those of $\psi(x)$ are as follows:

$$\frac{\overline{a_1^+}}{a_1^+} = -iP, \quad \frac{\overline{a_1^-}}{a_1^-} = iP, \quad \frac{\overline{a_2^+}}{a_2^+} = -N, \quad \frac{\overline{a_2^-}}{a_2^-} = N, \tag{9}$$

where

$$P = k_1\left(1 - \frac{\omega^2}{k_1^2 C_s^2} - \frac{F}{GA\kappa}\right), \quad N = k_2\left(1 + \frac{\omega^2}{k_2^2 C_s^2} - \frac{F}{GA\kappa}\right). \tag{9a}$$

3. The propagation, reflection and transmission of waves in axially loaded Timoshenko beams

From wave standpoint, vibrations propagating along a beam component are reflected and transmitted upon discontinuities and boundaries. The propagation is governed by the so-called propagation matrix. Consider two points A and B on a flexually vibrating uniform beam at distance x apart; denoting the positive- and negative-going wave vectors at points A and B as $\mathbf{a}^+$ and $\mathbf{a}^-$, and $\mathbf{b}^+$ and $\mathbf{b}^-$, respectively, they are related by

$$\mathbf{a}^- = \mathbf{f}(x)\mathbf{b}^-, \quad \mathbf{b}^+ = \mathbf{f}(x)\mathbf{a}^+, \tag{10}$$

where

$$\mathbf{a}^+ = \begin{Bmatrix} a_1^+ \\ a_2^+ \end{Bmatrix}, \quad \mathbf{a}^- = \begin{Bmatrix} a_1^- \\ a_2^- \end{Bmatrix}, \quad \mathbf{b}^+ = \begin{Bmatrix} b_1^+ \\ b_2^+ \end{Bmatrix}, \quad \mathbf{b}^- = \begin{Bmatrix} b_1^- \\ b_2^- \end{Bmatrix} \tag{10a}$$

and

$$\mathbf{f}(x) = \begin{bmatrix} e^{-ik_1 x} & 0 \\ 0 & e^{-k_2 x} \end{bmatrix} \tag{10b}$$

is known as the propagation matrix for a distance x.

The reflection and transmission characteristics are governed by the reflection and transmission matrices. The following derives the reflection and transmission matrices at discontinuities such as boundaries, cracks and cross-sectional changes.

3.1. Reflections at boundaries

A general boundary is shown in Fig. 1. The incident waves $\mathbf{a}^+$ give rise to reflected waves $\mathbf{a}^-$, which are related by

$$\mathbf{a}^- = \mathbf{r}\mathbf{a}^+. \tag{11}$$

The reflection matrix $\mathbf{r}$ can be determined by considering equilibrium at the boundary, that is

$$-EI\frac{\partial \psi}{\partial x} = K_R \psi_{\pm},$$

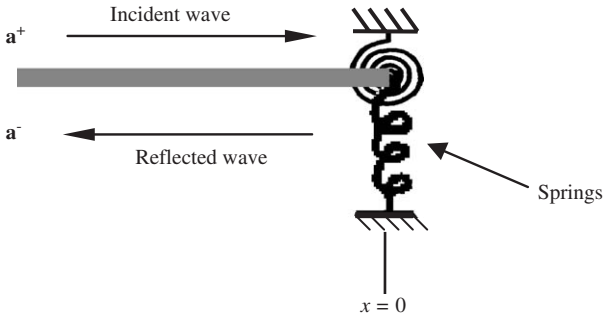

Fig. 1. A general boundary.

$$EI\frac{\partial^2\psi}{\partial x^2}+\rho I\omega^2\psi+F\frac{\partial y}{\partial x}=K_T y_{\pm}, \tag{12}$$

where K_T and K_R are the translational and rotational stiffnesses of the support, respectively, and

$$y=a_1^+\mathrm{e}^{-\mathrm{i}k_1x}+a_2^+\mathrm{e}^{-k_2x}+a_1^-\mathrm{e}^{\mathrm{i}k_1x}+a_2^-\mathrm{e}^{k_2x}, \tag{13a}$$

$$\psi=-\mathrm{i}Pa_1^+\mathrm{e}^{-\mathrm{i}k_1x}-Na_2^+\mathrm{e}^{-k_2x}+\mathrm{i}Pa_1^-\mathrm{e}^{\mathrm{i}k_1x}+Na_2^-\mathrm{e}^{k_2x}. \tag{13b}$$

If the boundary is at $x=0$, then the equilibrium conditions become

$$\boldsymbol{\alpha}_{11}\mathbf{a}^- -\boldsymbol{\alpha}_{12}\mathbf{a}^+=\mathbf{0}, \tag{14}$$

where

$$\boldsymbol{\alpha}_{11}=\begin{bmatrix} -EIPk_1+\mathrm{i}PK_R & EINk_2+NK_R \\ \mathrm{i}PEIk_1^2-\mathrm{i}P\rho I\omega^2-\mathrm{i}Fk_1+K_T & -NEIk_2^2-N\rho I\omega^2-Fk_2+K_T \end{bmatrix},$$

$$\boldsymbol{\alpha}_{12}=\begin{bmatrix} EIPk_1+\mathrm{i}PK_R & -EINk_2+NK_R \\ \mathrm{i}PEIk_1^2-\mathrm{i}P\rho I\omega^2-\mathrm{i}Fk_1-K_T & -NEIk_2^2-N\rho I\omega^2-Fk_2-K_T \end{bmatrix}.$$

From Eqs. (11) and (14), it follows that

$$\mathbf{r}=\boldsymbol{\alpha}_{12}^{-1}\boldsymbol{\alpha}_{11}. \tag{15}$$

Three common boundary conditions of interest are simply supported, clamped and free boundaries. Corresponding to these boundary conditions, K_T and K_R are either zero or infinite. The reflection matrices for simply supported, clamped and free boundary conditions are found as the following, respectively:

$$\mathbf{r}_s=\begin{bmatrix} -1 & 0 \\ 0 & -1 \end{bmatrix},$$

$$\mathbf{r}_c=\begin{bmatrix} \frac{P-\mathrm{i}N}{P+\mathrm{i}N} & \frac{-2\mathrm{i}N}{P+\mathrm{i}N} \\ \frac{-2P}{P+\mathrm{i}N} & -\frac{P-\mathrm{i}N}{P+\mathrm{i}N} \end{bmatrix}, \tag{16}$$

$$\mathbf{r}_f=\begin{bmatrix} \mathbf{r}_{f11} & \mathbf{r}_{f12} \\ \mathbf{r}_{f21} & \mathbf{r}_{f22} \end{bmatrix},$$

where

$$\mathbf{r}_{f11}=-\mathbf{r}_{f22}=-\frac{EIPNk_1k_2(k_2+\mathrm{i}k_1)+PN\rho I\omega^2(k_1-\mathrm{i}k_2)+Fk_1k_2(P-\mathrm{i}N)}{EIPNk_1k_2(k_2-\mathrm{i}k_1)+PN\rho I\omega^2(k_1+\mathrm{i}k_2)+Fk_1k_2(P+\mathrm{i}N)},$$

$$\mathbf{r}_{f12}=\frac{2Nk_2(EINk_2^2+\rho IN\omega^2+Fk_2)}{EIPNk_1k_2(k_2-\mathrm{i}k_1)+PN\rho I\omega^2(k_1+\mathrm{i}k_2)+Fk_1k_2(P+\mathrm{i}N)},$$

$$\mathbf{r}_{f21}=\frac{\mathrm{i}2Pk_1(-EIPk_1^2+\rho IP\omega^2+Fk_1)}{EIPNk_1k_2(k_2-\mathrm{i}k_1)+PN\rho I\omega^2(k_1+\mathrm{i}k_2)+Fk_1k_2(P+\mathrm{i}N)}.$$

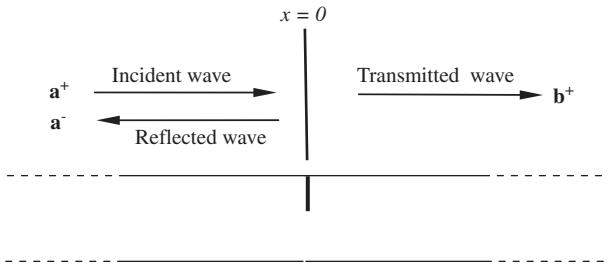

Fig. 2. A transverse open crack.

3.2. Crack

In this study, the local flexibility model from fracture mechanics is adopted, where the modification of stress field is assumed local. The continuous crack flexibility model distributes the added flexibility due to the crack over the length of a cracked beam [16]. In terms of modal response, results obtained from both models are in good agreement with experimental results.

Cracks could be open or breathing (open and close in time), depending on the loading conditions and vibration amplitudes. The open crack model is valid throughout the paper.

Considering an open crack at $x = 0$ as shown in Fig. 2, a set of positive-going waves $\mathbf{a}^+$ is incident upon the crack and gives rise to transmitted and reflected waves $\mathbf{b}^+$ and $\mathbf{a}^-$, which are related to the incident waves through the transmission and reflection matrices $\mathbf{t}$ and $\mathbf{r}$ by

$$\mathbf{b}^+ = \mathbf{t}\mathbf{a}^+, \quad \mathbf{a}^- = \mathbf{r}\mathbf{a}^+. \tag{17}$$

Denoting the transverse displacements and the slopes of the beam on the left- and right-hand sides of the crack as y_-, y_+, ψ_- and ψ_+, respectively, one has

$$y_- = a_1^+ e^{-ik_1 x} + a_2^+ e^{-k_2 x} + a_1^- e^{ik_1 x} + a_2^- e^{k_2 x}, \tag{18a}$$

$$y_+ = b_1^+ e^{-ik_1 x} + b_2^+ e^{-k_2 x}, \tag{18b}$$

$$\psi_- = -iPa_1^+ e^{-ik_1 x} - Na_2^+ e^{-k_2 x} + iPa_1^- e^{ik_1 x} + Na_2^- e^{k_2 x}, \tag{19a}$$

$$\psi_+ = -iPb_1^+ e^{-ik_1 x} - Nb_2^+ e^{-k_2 x}. \tag{19b}$$

Since the beam is continuous, one has

$$y_+ = y_-, \quad \psi_+ = \psi_- + CEI\frac{\partial \psi_-}{\partial x}. \tag{20}$$

where the term $CEI(\partial\psi_-/\partial x)$ represents a jump in the bending slope caused by local flexibility change at the crack and C is the so-called flexibility coefficient. C is related to crack size μ, which is defined as the ratio between the depth of the crack and the thickness of the beam, as shown by following [17]:

$$C = \frac{6\pi(1-\nu^2)h}{EI} f(\mu), \tag{21}$$

where

$$f(\mu) = 0.6272\mu^2 - 1.04533\mu^3 + 4.5948\mu^4 - 9.973\mu^5 + 20.2948\mu^6 - 33.0351\mu^7 + 47.1063\mu^8 - 40.7556\mu^9 + 19.6\mu^{10}. \tag{21a}$$

Writing the continuity conditions in matrix form, one has

$$\boldsymbol{\beta}_{11}\mathbf{b}^+ + \boldsymbol{\beta}_{12}\mathbf{a}^- = \boldsymbol{\beta}_{13}\mathbf{a}^+, \tag{22}$$

where

$$\boldsymbol{\beta}_{11} = \begin{bmatrix} 1 & 1 \\ -\mathrm{i}P & -N \end{bmatrix}, \ \boldsymbol{\beta}_{12} = \begin{bmatrix} -1 & -1 \\ -\mathrm{i}P + CEIPk_1 & -N - CEINk_2 \end{bmatrix},$$

$$\boldsymbol{\beta}_{13} = \begin{bmatrix} 1 & 1 \\ -\mathrm{i}P - CEIPk_1 & -N + CEINk_2 \end{bmatrix}. \tag{22a}$$

Furthermore, by considering the equilibrium of the support,

$$M_+ = M_-, \ \ V_+ = V_-, \tag{23}$$

one has

$$\boldsymbol{\beta}_{21}\mathbf{b}^+ + \boldsymbol{\beta}_{22}\mathbf{a}^- = \boldsymbol{\beta}_{23}\mathbf{a}^+, \tag{24}$$

where

$$\boldsymbol{\beta}_{21} = \begin{bmatrix} -EIPk_1 & EINk_2 \\ GA\kappa(-\mathrm{i}k_1 + \mathrm{i}P) + \mathrm{i}Fk_1 & GA\kappa(-k_2 + N) + Fk_2 \end{bmatrix},$$

$$\boldsymbol{\beta}_{22} = \begin{bmatrix} EIPk_1 & -EINk_2 \\ GA\kappa(-\mathrm{i}k_1 + \mathrm{i}P) + \mathrm{i}Fk_1 & GA\kappa(-k_2 + N) + Fk_2 \end{bmatrix},$$

$$\boldsymbol{\beta}_{23} = \begin{bmatrix} -EIPk_1 & EINk_2 \\ GA\kappa(-\mathrm{i}k_1 + \mathrm{i}P) + \mathrm{i}Fk_1 & GA\kappa(-k_2 + N) + Fk_2 \end{bmatrix}. \tag{24a}$$

Eqs. (17), (22) and (24) can be solved to obtain the reflection and transmission matrices at the crack discontinuity as

$$\mathbf{t} = \left(\boldsymbol{\beta}_{21} - \boldsymbol{\beta}_{22}\boldsymbol{\beta}_{12}^{-1}\boldsymbol{\beta}_{11}\right)^{-1}\left(\boldsymbol{\beta}_{23} - \boldsymbol{\beta}_{22}\boldsymbol{\beta}_{12}^{-1}\boldsymbol{\beta}_{13}\right),$$
$$\mathbf{r} = \left(\boldsymbol{\beta}_{22} - \boldsymbol{\beta}_{21}\boldsymbol{\beta}_{11}^{-1}\boldsymbol{\beta}_{12}\right)^{-1}\left(\boldsymbol{\beta}_{23} - \boldsymbol{\beta}_{21}\boldsymbol{\beta}_{11}^{-1}\boldsymbol{\beta}_{13}\right). \tag{25}$$

3.3. Change in section

Let two beams of different properties be joined at $x = 0$ as shown in Fig. 3. Due to impedance mismatching, incident waves from one beam give rise to reflected and transmitted waves at the junction. However, the displacement, slope, bending moment and shear force are all continuous at the junction. The reflection and transmission matrices can then be obtained from the continuity and equilibrium conditions.

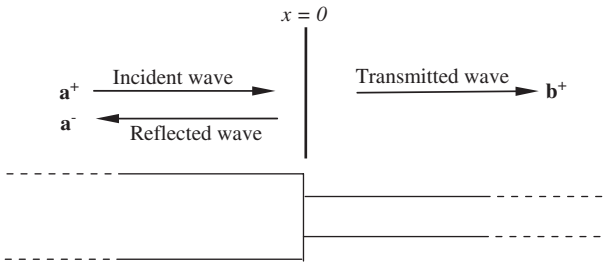

Fig. 3. A step change.

Denoting the parameters related to the incident and transmitted sides of the junction with subscripts L and R, respectively, choosing the origin at the point where the section changes, at $x = 0$, one has

$$y_L = y_R, \quad \psi_L = \psi_R, \quad M_L = M_R, \quad V_L = V_R. \tag{26}$$

Considering Eq. (17), Eq. (26) can be put into matrix form in terms of the reflection and the transmission matrices $\mathbf{r}_{LL}$ and $\mathbf{t}_{LR}$:

$$\gamma_{11}\mathbf{r}_{LL} + \gamma_{12}\mathbf{t}_{LR} = \gamma_{13}, \;\; \gamma_{21}\mathbf{r}_{LL} + \gamma_{22}\mathbf{t}_{LR} = \gamma_{23}, \tag{27}$$

where

$$\gamma_{11} = \begin{bmatrix} 1 & 1 \\ \mathrm{i}P_L & N_L \end{bmatrix}, \;\; \gamma_{12} = \begin{bmatrix} -1 & -1 \\ \mathrm{i}P_R & N_R \end{bmatrix}, \;\; \gamma_{13} = \begin{bmatrix} -1 & -1 \\ \mathrm{i}P_L & N_L \end{bmatrix},$$

$$\gamma_{21} = \begin{bmatrix} -(EI)_L P_L k_{L1} & (EI)_L N_L k_{L2} \\ \mathrm{i}(EI)_L P_L k_{L1}^2 - \mathrm{i}\rho I\omega^2 P_L - \mathrm{i}Fk_{L1} & -(EI)_L N_L k_{L2}^2 - \rho I\omega^2 N_L - Fk_{L2} \end{bmatrix}, \tag{27a}$$

$$\gamma_{22} = \begin{bmatrix} (EI)_R P_R k_{R1} & -(EI)_R N_R k_{R2} \\ \mathrm{i}(EI)_R P_R k_{R1}^2 - \mathrm{i}\rho I\omega^2 P_R - \mathrm{i}Fk_{R1} & -(EI)_R N_R k_{R2}^2 - \rho I\omega^2 N_R - Fk_{R2} \end{bmatrix},$$

$$\gamma_{23} = \begin{bmatrix} (EI)_L P_L k_{L1} & -(EI)_L N_L k_{L2} \\ \mathrm{i}(EI)_L P_L k_{L1}^2 - \mathrm{i}\rho I\omega^2 P_L - \mathrm{i}Fk_{L1} & -(EI)_L N_L k_{L2}^2 - \rho I\omega^2 N_L - Fk_{L2} \end{bmatrix}.$$

The equations can be solved for the reflection and transmission matrices $\mathbf{r}_{LL}$ and $\mathbf{t}_{LR}$, which are given as

$$\begin{aligned} \mathbf{r}_{LL} &= \left(\gamma_{12}^{-1}\gamma_{11} - \gamma_{22}^{-1}\gamma_{21}\right)^{-1}\left(\gamma_{12}^{-1}\gamma_{13} - \gamma_{22}^{-1}\gamma_{23}\right), \\ \mathbf{t}_{LR} &= \left(\gamma_{11}^{-1}\gamma_{12} - \gamma_{21}^{-1}\gamma_{22}\right)^{-1}\left(\gamma_{11}^{-1}\gamma_{13} - \gamma_{21}^{-1}\gamma_{23}\right). \end{aligned} \tag{28}$$

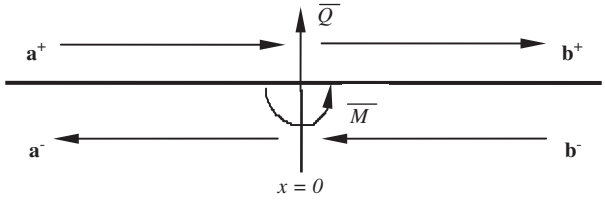

Fig. 4. Force-generated waves.

4. Waves generated by externally applied point forces and moments

Applied forces and moments have the effect of injecting waves into a structure. Consider the flexural waves injected into a thin beam by a point force $\overline{Q}$ and moment $\overline{M}$ applied at $x = 0$ as shown in Fig. 4. At $x = 0$, there are discontinuities in the shear force and bending moment in the beam with resulting discontinuities in the waves **a** and **b** on either sides of the excitation point. The relations between the applied forces and the waves are described by the following continuity and equilibrium conditions:

$$\begin{aligned} &y_- = y_+, \;\; \psi_- = \psi_+, \\ &\overline{Q} = \left(-EI\tfrac{\partial^2\psi_-}{\partial x^2} - \rho I\omega^2\psi_- - F\tfrac{\partial y_-}{\partial x}\right) - \left(-EI\tfrac{\partial^2\psi_+}{\partial x^2} - \rho I\omega^2\psi_+ - F\tfrac{\partial y_+}{\partial x}\right), \\ &\overline{M} = EI\left(\tfrac{\partial\psi_-}{\partial x} - \tfrac{\partial\psi_+}{\partial x}\right), \end{aligned} \tag{29}$$

where

$$\begin{aligned} y_- &= a_1^+ e^{-ik_1x} + a_2^+ e^{-k_2x} + a_1^- e^{ik_1x} + a_2^- e^{k_2x}, \\ y_+ &= b_1^+ e^{-ik_1x} + b_2^+ e^{-k_2x} + b_1^- e^{ik_1x} + b_2^- e^{k_2x}, \\ \psi_- &= -iPa_1^+ e^{-ik_1x} - Na_2^+ e^{-k_2x} + iPa_1^- e^{ik_1x} + Na_2^- e^{k_2x}, \\ \psi_+ &= -iPb_1^+ e^{-ik_1x} - Nb_2^+ e^{-k_2x} + iPb_1^- e^{ik_1x} + Nb_2^- e^{k_2x}. \end{aligned} \tag{29a}$$

The continuity and the equilibrium conditions can be written in matrix form as

$$\begin{aligned} \boldsymbol{\delta}_{11}\mathbf{b}_1^+ + \boldsymbol{\delta}_{12}\mathbf{b}_1^- + \boldsymbol{\delta}_{13}\mathbf{a}_1^+ + \boldsymbol{\delta}_{14}\mathbf{a}_1^- &= \mathbf{0}, \\ \boldsymbol{\delta}_{21}\mathbf{b}_1^+ + \boldsymbol{\delta}_{22}\mathbf{b}_1^- + \boldsymbol{\delta}_{23}\mathbf{a}_1^+ + \boldsymbol{\delta}_{24}\mathbf{a}_1^- &= \mathbf{q}, \end{aligned} \tag{30}$$

where $\mathbf{q} = \begin{bmatrix} \overline{M} & \overline{Q} \end{bmatrix}^{\mathrm{T}}$ and

$$\boldsymbol{\delta}_{11} = -\boldsymbol{\delta}_{13} = \begin{bmatrix} iP & N \\ -1 & -1 \end{bmatrix}, \;\; \boldsymbol{\delta}_{12} = -\boldsymbol{\delta}_{14} = \begin{bmatrix} -iP & -N \\ -1 & -1 \end{bmatrix},$$

$$\boldsymbol{\delta}_{21} = -\boldsymbol{\delta}_{23} = \begin{bmatrix} EIPk_1 & -EINk_2 \\ iEIPk_1^2 - i\rho I\omega^2 P - iFk_1 & -EINk_2^2 - \rho I\omega^2 N - Fk_2 \end{bmatrix}, \tag{30a}$$

$$\boldsymbol{\delta}_{22} = -\boldsymbol{\delta}_{24} = \begin{bmatrix} EIPk_1 & -EINk_2 \\ -iEIPk_1^2 + i\rho I\omega^2 P + iFk_1 & EINk_2^2 + \rho I\omega^2 N + Fk_2 \end{bmatrix},$$

from which it follows that

$$\mathbf{b}^+ - \mathbf{a}^+ = \mathbf{q}^+, \quad \mathbf{b}^- - \mathbf{a}^- = \mathbf{q}^-, \tag{31}$$

where

$$\begin{aligned} \mathbf{q}^+ &= -\left(\boldsymbol{\delta}_{12}^{-1}\boldsymbol{\delta}_{11} - \boldsymbol{\delta}_{22}^{-1}\boldsymbol{\delta}_{21}\right) \text{ on, } \boldsymbol{\delta}_{22}^{-1}\mathbf{q}, \\ \mathbf{q}^- &= -\left(\boldsymbol{\delta}_{11}^{-1}\boldsymbol{\delta}_{12} - \boldsymbol{\delta}_{21}^{-1}\boldsymbol{\delta}_{22}\right) \text{ on, } \boldsymbol{\delta}_{21}^{-1}\mathbf{q}. \end{aligned} \tag{31a}$$

5. Vibration analysis using wave approach

The transmission and reflection matrices for waves incident upon various discontinuities were derived above. The waves injected by externally applied forces/moments were also found in matrix form. These matrices can be combined to provide a concise and systematic approach for vibration analyses of axially loaded Timoshenko beams. The systematic approach is illustrated through free and forced vibration analyses of two example cantilevered cracked beams, namely, a uniform and a stepped Timoshenko beam. The physical parameters of the beam are listed in Table 1.

5.1. Free vibration analysis

(i) *A uniform beam with a crack*

Fig. 5 shows a uniform cracked Timoshenko beam. The geometric discontinuity is at point D. The incident and reflected waves at the clamped boundary A, free boundary B and the left- and right-hand sides of D are denoted by $\mathbf{a}^{\mp}$, $\mathbf{b}^{\pm}$, $\mathbf{d}_2^{\pm}$ and $\mathbf{d}_3^{\mp}$, respectively. The relationships between the incident and the reflected waves at the boundaries are described as:

$$\mathbf{a}^+ = \mathbf{r}_a\mathbf{a}^-, \quad \mathbf{b}^- = \mathbf{r}_b\mathbf{b}^+, \tag{32}$$

At the geometric discontinuity D, the incident, the reflected and the transmitted waves are related as follows:

$$\mathbf{d}_2^- = \mathbf{r}\mathbf{d}_2^+ + \mathbf{t}\mathbf{d}_3^-, \quad \mathbf{d}_3^+ = \mathbf{r}\mathbf{d}_3^- + \mathbf{t}\mathbf{d}_2^+, \tag{33}$$

where $\mathbf{r}$ and $\mathbf{t}$ are the reflection and the transmission matrices of the crack, as discussed in Section 3.2.

Table 1
Physical parameters of the example beam

Rigidities			Polar mass moment of inertia (kg m)	
Shear: $GA\kappa$ (N)	Bending: EI (Nm^2)	Torsion: GJ (Nm^2)		
6343.3	0.2865	0.1891	0.777×10^{-6}	
Mass per unit length (kg/m)	Width: b(m)	Depth: h(m)	Length: L(m)	Poisson's ratio
0.0544	0.0127	0.00318	0.1905	0.29

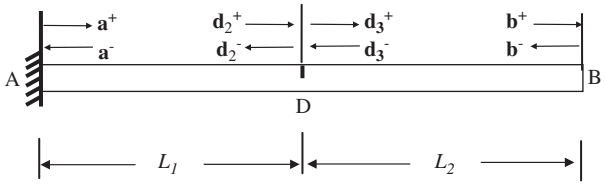

Fig. 5. A cracked cantilever beam.

The propagation relations are

$$\mathbf{d}_2^+ = \mathbf{f}(L_1)\mathbf{a}^+,\ \ \mathbf{a}^- = \mathbf{f}(L_1)\mathbf{d}_2^-,\ \ \mathbf{b}^+ = \mathbf{f}(L_2)\mathbf{d}_3^+,\ \ \mathbf{d}_3^- = \mathbf{f}(L_2)\mathbf{b}^-, \tag{34}$$

where $\mathbf{f}(L_1)$ and $\mathbf{f}(L_2)$ are the propagation matrices between AD and DB, respectively.

Writing Eqs. (32)–(34) in matrix form gives

$$\begin{bmatrix} -\mathbf{I} & \mathbf{r}_a & \mathbf{0} & \mathbf{0} & \mathbf{0} & \mathbf{0} & \mathbf{0} & \mathbf{0} \\ \mathbf{0} & \mathbf{0} & \mathbf{0} & \mathbf{0} & \mathbf{0} & \mathbf{0} & \mathbf{r}_b & -\mathbf{I} \\ \mathbf{0} & \mathbf{0} & \mathbf{r} & -\mathbf{I} & \mathbf{0} & \mathbf{t} & \mathbf{0} & \mathbf{0} \\ \mathbf{0} & \mathbf{0} & \mathbf{t} & \mathbf{0} & -\mathbf{I} & \mathbf{r} & \mathbf{0} & \mathbf{0} \\ \mathbf{f}(L_1) & \mathbf{0} & -\mathbf{I} & \mathbf{0} & \mathbf{0} & \mathbf{0} & \mathbf{0} & \mathbf{0} \\ \mathbf{0} & -\mathbf{I} & \mathbf{0} & \mathbf{f}(L_1) & \mathbf{0} & \mathbf{0} & \mathbf{0} & \mathbf{0} \\ \mathbf{0} & \mathbf{0} & \mathbf{0} & \mathbf{0} & \mathbf{f}(L_2) & \mathbf{0} & -\mathbf{I} & \mathbf{0} \\ \mathbf{0} & \mathbf{0} & \mathbf{0} & \mathbf{0} & \mathbf{0} & -\mathbf{I} & \mathbf{0} & \mathbf{f}(L_2) \end{bmatrix} \begin{bmatrix} \mathbf{a}^+ \\ \mathbf{a}^- \\ \mathbf{d}_2^+ \\ \mathbf{d}_2^- \\ \mathbf{d}_3^+ \\ \mathbf{d}_3^- \\ \mathbf{b}^+ \\ \mathbf{b}^- \end{bmatrix} = \mathbf{0}. \tag{35}$$

For a non-trivial solution, it follows that

$$\begin{vmatrix} -\mathbf{I} & \mathbf{r}_a & \mathbf{0} & \mathbf{0} & \mathbf{0} & \mathbf{0} & \mathbf{0} & \mathbf{0} \\ \mathbf{0} & \mathbf{0} & \mathbf{0} & \mathbf{0} & \mathbf{0} & \mathbf{0} & \mathbf{r}_b & -\mathbf{I} \\ \mathbf{0} & \mathbf{0} & \mathbf{r} & -\mathbf{I} & \mathbf{0} & \mathbf{t} & \mathbf{0} & \mathbf{0} \\ \mathbf{0} & \mathbf{0} & \mathbf{t} & \mathbf{0} & -\mathbf{I} & \mathbf{r} & \mathbf{0} & \mathbf{0} \\ \mathbf{f}(L_1) & \mathbf{0} & -\mathbf{I} & \mathbf{0} & \mathbf{0} & \mathbf{0} & \mathbf{0} & \mathbf{0} \\ \mathbf{0} & -\mathbf{I} & \mathbf{0} & \mathbf{f}(L_1) & \mathbf{0} & \mathbf{0} & \mathbf{0} & \mathbf{0} \\ \mathbf{0} & \mathbf{0} & \mathbf{0} & \mathbf{0} & \mathbf{f}(L_2) & \mathbf{0} & -\mathbf{I} & \mathbf{0} \\ \mathbf{0} & \mathbf{0} & \mathbf{0} & \mathbf{0} & \mathbf{0} & -\mathbf{I} & \mathbf{0} & \mathbf{f}(L_2) \end{vmatrix} = \mathbf{0}. \tag{36}$$

Eq. (36) is the characteristic equation from which the natural frequencies of the uniform cracked Timoshenko beam can be found.

The natural frequencies of the example beam with and without axial loading and with and without crack are listed in Table 2. The crack is assumed to be at $0.5L$. The values of the natural frequencies are obtained through a self-written program in Matlab environment by recording simultaneous sign changes in both real and imaginary responses. The precision of the parameters can be as high as machine precision. Here the step size is chosen as 0.1 Hz. It can be seen from

Table 2
Natural frequencies (Hz) of the uniform beam under various axial loadings and with varying crack ratios μ

Mode number	Crack ratio $\mu = 0$			Crack ratio $\mu = 0.3$			Crack ratio $\mu = 0.5$		
	0 N	+15 N	−15 N	0 N	+15 N	−15 N	0 N	+15 N	−15 N
1	35.3	27.9	46.8	35.2	27.7	46.8	34.9	27.3	46.8
2	217.4	167.7	227.4	214.3	163.6	224.3	207.0	153.8	217.1
3	592.6	520.7	614.5	592.6	520.6	614.4	592.5	520.6	614.3

Table 3
Natural frequencies (Hz) of the uniform beam at various crack locations

Mode number	Crack ratio $\mu = 0.3$ (Crack located at $0.3L$)			Crack ratio $\mu = 0.3$ (Crack located at $0.5L$)			Crack ratio $\mu = 0.3$ (Crack located at $0.8L$)		
	0 N	+15 N	−15 N	0 N	+15 N	−15 N	0 N	+15 N	−15 N
1	34.1	25.1	46.0	35.2	27.7	46.8	35.3	28.6	46.8
2	215.2	165.2	225.0	214.3	163.6	224.3	215.4	165.5	226.0
3	571.2	495.8	592.8	592.6	520.6	614.4	572.2	497.0	594.5

Table 2 that both an axial loading and a crack have the effects of shifting the natural frequencies. A tensile loading in general increases the natural frequencies, while a compressive loading decreases the natural frequencies. Regardless of the loading situation, a crack is seen to decrease the natural frequencies. Thus, it has the effect of "softening" the structure; the deeper the crack, the softer the structure.

Table 3 lists the natural frequencies of the example beam corresponding to various crack locations. It shows that the location of a crack affects the free vibration frequencies of a structure.

(ii) *A stepped beam with a crack*

Fig. 6 shows a cracked stepped Timoshenko beam. The step discontinuity is at point E. The analysis follows the same procedures as described above, except that there is additional wave reflection and transmission at the step change. Waves on both sides of the step discontinuity are related as the following:

$$\mathbf{e}_3^- = \mathbf{r}_{LL}\mathbf{e}_3^+ + \mathbf{t}_{RL}\mathbf{e}_4^-, \quad \mathbf{e}_4^+ = \mathbf{r}_{RR}\mathbf{e}_4^- + \mathbf{t}_{LR}\mathbf{e}_3^+, \tag{37}$$

The subscripts of $\mathbf{r}$ and $\mathbf{t}$ identify the incident and transmitted sides of the junction.

The propagation relations are redefined as

$$\begin{aligned} &\mathbf{d}_2^+ = \mathbf{f}(L_1)\mathbf{a}^+, \ \ \mathbf{a}^- = \mathbf{f}(L_1)\mathbf{d}_2^-, \ \ \mathbf{e}_3^+ = \mathbf{f}(L_2)\mathbf{d}_3^+, \\ &\mathbf{d}_3^- = \mathbf{f}(L_2)\mathbf{e}_3^-, \ \ \mathbf{b}^+ = \mathbf{f}(L_3)\mathbf{e}_4^+, \ \ \mathbf{e}_4^- = \mathbf{f}(L_3)\mathbf{b}^-, \end{aligned} \tag{38}$$

where $\mathbf{f}(L_1)$, $\mathbf{f}(L_2)$ and $\mathbf{f}(L_3)$ are the propagation matrices between AD, DE and EB, respectively.

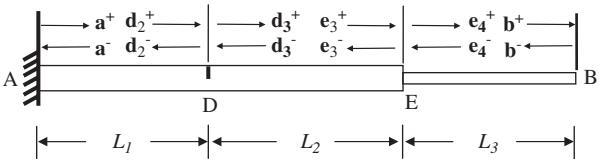

Fig. 6. A cracked stepped cantilever beam.

Writing Eqs. (32), (37) and (38) in matrix form gives

$$\begin{bmatrix} -\mathbf{I} & \mathbf{r}_a & \mathbf{0} & \mathbf{0} & \mathbf{0} & \mathbf{0} & \mathbf{0} & \mathbf{0} & \mathbf{0} & \mathbf{0} & \mathbf{0} & \mathbf{0} \\ \mathbf{0} & \mathbf{0} & \mathbf{0} & \mathbf{0} & \mathbf{0} & \mathbf{0} & \mathbf{0} & \mathbf{0} & \mathbf{0} & \mathbf{0} & \mathbf{r}_b & -\mathbf{I} \\ \mathbf{0} & \mathbf{0} & \mathbf{r} & -\mathbf{I} & \mathbf{0} & \mathbf{t} & \mathbf{0} & \mathbf{0} & \mathbf{0} & \mathbf{0} & \mathbf{0} & \mathbf{0} \\ \mathbf{0} & \mathbf{0} & \mathbf{t} & \mathbf{0} & -\mathbf{I} & \mathbf{r} & \mathbf{0} & \mathbf{0} & \mathbf{0} & \mathbf{0} & \mathbf{0} & \mathbf{0} \\ \mathbf{0} & \mathbf{0} & \mathbf{0} & \mathbf{0} & \mathbf{0} & \mathbf{0} & \mathbf{r}_{LL} & -\mathbf{I} & \mathbf{0} & \mathbf{t}_{RL} & \mathbf{0} & \mathbf{0} \\ \mathbf{0} & \mathbf{0} & \mathbf{0} & \mathbf{0} & \mathbf{0} & \mathbf{0} & \mathbf{t}_{LR} & \mathbf{0} & -\mathbf{I} & \mathbf{r}_{RR} & \mathbf{0} & \mathbf{0} \\ \mathbf{f}(L_1) & \mathbf{0} & -\mathbf{I} & \mathbf{0} & \mathbf{0} & \mathbf{0} & \mathbf{0} & \mathbf{0} & \mathbf{0} & \mathbf{0} & \mathbf{0} & \mathbf{0} \\ \mathbf{0} & -\mathbf{I} & \mathbf{0} & \mathbf{f}(L_1) & \mathbf{0} & \mathbf{0} & \mathbf{0} & \mathbf{0} & \mathbf{0} & \mathbf{0} & \mathbf{0} & \mathbf{0} \\ \mathbf{0} & \mathbf{0} & \mathbf{0} & \mathbf{0} & \mathbf{f}(L_2) & \mathbf{0} & -\mathbf{I} & \mathbf{0} & \mathbf{0} & \mathbf{0} & \mathbf{0} & \mathbf{0} \\ \mathbf{0} & \mathbf{0} & \mathbf{0} & \mathbf{0} & \mathbf{0} & -\mathbf{I} & \mathbf{0} & \mathbf{f}(L_2) & \mathbf{0} & \mathbf{0} & \mathbf{0} & \mathbf{0} \\ \mathbf{0} & \mathbf{0} & \mathbf{0} & \mathbf{0} & \mathbf{0} & \mathbf{0} & \mathbf{0} & \mathbf{0} & \mathbf{f}(L_3) & \mathbf{0} & -\mathbf{I} & \mathbf{0} \\ \mathbf{0} & \mathbf{0} & \mathbf{0} & \mathbf{0} & \mathbf{0} & \mathbf{0} & \mathbf{0} & \mathbf{0} & \mathbf{0} & -\mathbf{I} & \mathbf{0} & \mathbf{f}(L_3) \end{bmatrix} \begin{bmatrix} \mathbf{a}^+ \\ \mathbf{a}^- \\ \mathbf{d}_2^+ \\ \mathbf{d}_2^- \\ \mathbf{d}_3^+ \\ \mathbf{d}_3^- \\ \mathbf{e}_3^+ \\ \mathbf{e}_3^- \\ \mathbf{e}_4^+ \\ \mathbf{e}_4^- \\ \mathbf{b}^+ \\ \mathbf{b}^- \end{bmatrix} = \begin{bmatrix} \mathbf{0} \\ \mathbf{0} \\ \mathbf{0} \\ \mathbf{0} \\ \mathbf{0} \\ \mathbf{0} \\ \mathbf{0} \\ \mathbf{0} \\ \mathbf{0} \\ \mathbf{0} \\ \mathbf{0} \\ \mathbf{0} \end{bmatrix}. \tag{39}$$

For a non-trivial solution, it follows that

$$\begin{vmatrix} -\mathbf{I} & \mathbf{r}_a & \mathbf{0} & \mathbf{0} & \mathbf{0} & \mathbf{0} & \mathbf{0} & \mathbf{0} & \mathbf{0} & \mathbf{0} & \mathbf{0} & \mathbf{0} \\ \mathbf{0} & \mathbf{0} & \mathbf{0} & \mathbf{0} & \mathbf{0} & \mathbf{0} & \mathbf{0} & \mathbf{0} & \mathbf{0} & \mathbf{0} & \mathbf{r}_b & -\mathbf{I} \\ \mathbf{0} & \mathbf{0} & \mathbf{r} & -\mathbf{I} & \mathbf{0} & \mathbf{t} & \mathbf{0} & \mathbf{0} & \mathbf{0} & \mathbf{0} & \mathbf{0} & \mathbf{0} \\ \mathbf{0} & \mathbf{0} & \mathbf{t} & \mathbf{0} & -\mathbf{I} & \mathbf{r} & \mathbf{0} & \mathbf{0} & \mathbf{0} & \mathbf{0} & \mathbf{0} & \mathbf{0} \\ \mathbf{0} & \mathbf{0} & \mathbf{0} & \mathbf{0} & \mathbf{0} & \mathbf{0} & \mathbf{r}_{LL} & -\mathbf{I} & \mathbf{0} & \mathbf{t}_{RL} & \mathbf{0} & \mathbf{0} \\ \mathbf{0} & \mathbf{0} & \mathbf{0} & \mathbf{0} & \mathbf{0} & \mathbf{0} & \mathbf{t}_{LR} & \mathbf{0} & -\mathbf{I} & \mathbf{r}_{RR} & \mathbf{0} & \mathbf{0} \\ \mathbf{f}(L_1) & \mathbf{0} & -\mathbf{I} & \mathbf{0} & \mathbf{0} & \mathbf{0} & \mathbf{0} & \mathbf{0} & \mathbf{0} & \mathbf{0} & \mathbf{0} & \mathbf{0} \\ \mathbf{0} & -\mathbf{I} & \mathbf{0} & \mathbf{f}(L_1) & \mathbf{0} & \mathbf{0} & \mathbf{0} & \mathbf{0} & \mathbf{0} & \mathbf{0} & \mathbf{0} & \mathbf{0} \\ \mathbf{0} & \mathbf{0} & \mathbf{0} & \mathbf{0} & \mathbf{f}(L_2) & \mathbf{0} & -\mathbf{I} & \mathbf{0} & \mathbf{0} & \mathbf{0} & \mathbf{0} & \mathbf{0} \\ \mathbf{0} & \mathbf{0} & \mathbf{0} & \mathbf{0} & \mathbf{0} & -\mathbf{I} & \mathbf{0} & \mathbf{f}(L_2) & \mathbf{0} & \mathbf{0} & \mathbf{0} & \mathbf{0} \\ \mathbf{0} & \mathbf{0} & \mathbf{0} & \mathbf{0} & \mathbf{0} & \mathbf{0} & \mathbf{0} & \mathbf{0} & \mathbf{f}(L_3) & \mathbf{0} & -\mathbf{I} & \mathbf{0} \\ \mathbf{0} & \mathbf{0} & \mathbf{0} & \mathbf{0} & \mathbf{0} & \mathbf{0} & \mathbf{0} & \mathbf{0} & \mathbf{0} & -\mathbf{I} & \mathbf{0} & \mathbf{f}(L_3) \end{vmatrix} = \mathbf{0}. \tag{40}$$

Table 4
Natural frequencies (Hz) of the stepped beam under various axial loadings and with varying crack ratios μ

Mode number	Crack ratio $\mu = 0$			Crack ratio $\mu = 0.3$			Crack ratio $\mu = 0.5$		
	0 N	+15 N	−15 N	0 N	+15 N	−15 N	0 N	+15 N	−15 N
1	37.7	31.4	50.1	37.6	31.3	50.1	37.3	31.0	50.1
2	209.8	156.3	222.5	207.2	152.9	219.9	201.2	144.3	213.7
3	551.7	471.2	572.1	551.6	470.1	572.0	551.3	470.4	571.8

Eq. (40) gives the characteristic equation from which the natural frequencies of the cracked stepped Timoshenko beam can be found.

The natural frequencies of the example beam with and without axial loading and with and without crack are listed in Table 4. The crack is still assumed to be at $0.5L$, and the step change is assumed at $0.6L$. The step is assumed to be a thickness change of 0.85 (right/left). The values of the natural frequencies are obtained through a self-written program in Matlab environment by recording simultaneous sign changes in both real and imaginary responses. The step size is chosen to be 0.1 Hz. Again, a tensile loading is seen to increase the natural frequencies, while a compressive loading decreases the natural frequencies and a crack has the effect of "softening" the structure, as observed earlier for the uniform beam.

5.2. Forced vibration analysis

(i) *A uniform beam with a crack*

Fig. 7 shows the cracked uniform beam with a point force and a moment applied at point C. The wave amplitudes at the boundaries and the crack discontinuity are the same as described in Section 5.1(i); the propagation relations are redefined as the following:

$$\begin{aligned} &\mathbf{c}_1^+ = \mathbf{f}(L_{11})\mathbf{a}^+, \quad \mathbf{a}^- = \mathbf{f}(L_{11})\mathbf{c}_1^-, \quad \mathbf{d}_2^+ = \mathbf{f}(L_{12})\mathbf{c}_2^+, \\ &\mathbf{c}_2^- = \mathbf{f}(L_{12})\mathbf{d}_2^-, \quad \mathbf{b}^+ = \mathbf{f}(L_2)\mathbf{d}_3^+, \quad \mathbf{d}_3^- = \mathbf{f}(L_2)\mathbf{b}^-, \end{aligned} \tag{41}$$

where $\mathbf{f}(L_{11})$ and $\mathbf{f}(L_{12})$ are the propagation matrices between AC and CD, respectively. Waves generated by the applied point force and moment are related to each other as described in Section 4, that is,

$$\mathbf{c}_2^+ - \mathbf{c}_1^+ = \mathbf{q}^+, \quad \mathbf{c}_2^- - \mathbf{c}_1^- = \mathbf{q}^-. \tag{42}$$

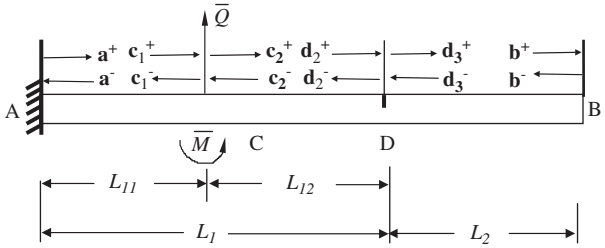

Fig. 7. A cracked cantilever beam with applied force and moment.

Writing Eqs. (32), (33), (41) and (42) in matrix form gives

$$\begin{bmatrix}
-\mathbf{I} & \mathbf{r}_a & \mathbf{0} & \mathbf{0} & \mathbf{0} & \mathbf{0} & \mathbf{0} & \mathbf{0} & \mathbf{0} & \mathbf{0} & \mathbf{0} & \mathbf{0} \\
\mathbf{0} & \mathbf{0} & \mathbf{0} & \mathbf{0} & \mathbf{0} & \mathbf{0} & \mathbf{0} & \mathbf{0} & \mathbf{0} & \mathbf{0} & \mathbf{r}_b & -\mathbf{I} \\
\mathbf{0} & \mathbf{0} & \mathbf{0} & \mathbf{0} & \mathbf{0} & \mathbf{0} & \mathbf{r} & -\mathbf{I} & \mathbf{0} & \mathbf{t} & \mathbf{0} & \mathbf{0} \\
\mathbf{0} & \mathbf{0} & \mathbf{0} & \mathbf{0} & \mathbf{0} & \mathbf{0} & \mathbf{t} & \mathbf{0} & -\mathbf{I} & \mathbf{r} & \mathbf{0} & \mathbf{0} \\
\mathbf{0} & \mathbf{0} & -\mathbf{I} & \mathbf{0} & \mathbf{I} & \mathbf{0} & \mathbf{0} & \mathbf{0} & \mathbf{0} & \mathbf{0} & \mathbf{0} & \mathbf{0} \\
\mathbf{0} & \mathbf{0} & \mathbf{0} & -\mathbf{I} & \mathbf{0} & \mathbf{I} & \mathbf{0} & \mathbf{0} & \mathbf{0} & \mathbf{0} & \mathbf{0} & \mathbf{0} \\
\mathbf{f}(L_{11}) & \mathbf{0} & -\mathbf{I} & \mathbf{0} & \mathbf{0} & \mathbf{0} & \mathbf{0} & \mathbf{0} & \mathbf{0} & \mathbf{0} & \mathbf{0} & \mathbf{0} \\
\mathbf{0} & -\mathbf{I} & \mathbf{0} & \mathbf{f}(L_{11}) & \mathbf{0} & \mathbf{0} & \mathbf{0} & \mathbf{0} & \mathbf{0} & \mathbf{0} & \mathbf{0} & \mathbf{0} \\
\mathbf{0} & \mathbf{0} & \mathbf{0} & \mathbf{0} & \mathbf{f}(L_{12}) & \mathbf{0} & -\mathbf{I} & \mathbf{0} & \mathbf{0} & \mathbf{0} & \mathbf{0} & \mathbf{0} \\
\mathbf{0} & \mathbf{0} & \mathbf{0} & \mathbf{0} & \mathbf{0} & -\mathbf{I} & \mathbf{0} & \mathbf{f}(L_{12}) & \mathbf{0} & \mathbf{0} & \mathbf{0} & \mathbf{0} \\
\mathbf{0} & \mathbf{0} & \mathbf{0} & \mathbf{0} & \mathbf{0} & \mathbf{0} & \mathbf{0} & \mathbf{0} & \mathbf{f}(L_2) & \mathbf{0} & -\mathbf{I} & \mathbf{0} \\
\mathbf{0} & \mathbf{0} & \mathbf{0} & \mathbf{0} & \mathbf{0} & \mathbf{0} & \mathbf{0} & \mathbf{0} & \mathbf{0} & -\mathbf{I} & \mathbf{0} & \mathbf{f}(L_2)
\end{bmatrix}
\begin{bmatrix}
\mathbf{a}^+ \\ \mathbf{a}^- \\ \mathbf{c}_1^+ \\ \mathbf{c}_1^- \\ \mathbf{c}_2^+ \\ \mathbf{c}_2^- \\ \mathbf{d}_2^+ \\ \mathbf{d}_2^- \\ \mathbf{d}_3^+ \\ \mathbf{d}_3^- \\ \mathbf{b}^+ \\ \mathbf{b}^-
\end{bmatrix}
=
\begin{bmatrix}
\mathbf{0} \\ \mathbf{0} \\ \mathbf{0} \\ \mathbf{0} \\ \mathbf{q}^+ \\ \mathbf{q}^- \\ \mathbf{0} \\ \mathbf{0} \\ \mathbf{0} \\ \mathbf{0} \\ \mathbf{0} \\ \mathbf{0}
\end{bmatrix}, \tag{43}$$

from which the magnitudes of the waves can be solved in terms of the external excitations, and the deflection of any point along the beam can then be found. For example, the deflection of a point in region 1 that is a distance x from the excitation point is given by

$$\begin{aligned}
y_- &= \begin{bmatrix} 1 & 1 \end{bmatrix} \mathbf{f}(x)\mathbf{c}_1^- + \begin{bmatrix} 1 & 1 \end{bmatrix} \mathbf{f}(-x)\mathbf{c}_1^+, \\
y_+ &= \begin{bmatrix} 1 & 1 \end{bmatrix} \mathbf{f}(x)\mathbf{c}_2^+ + \begin{bmatrix} 1 & 1 \end{bmatrix} \mathbf{f}(-x)\mathbf{c}_2^-.
\end{aligned} \tag{44}$$

Fig. 8 shows the frequency responses of the cracked uniform beam due to a point force excitation at $0.75L$, with a disturbance force applied at $0.45L$ from the clamped end. The resonances are seen to occur at the natural frequencies as those predicted in Table 2.

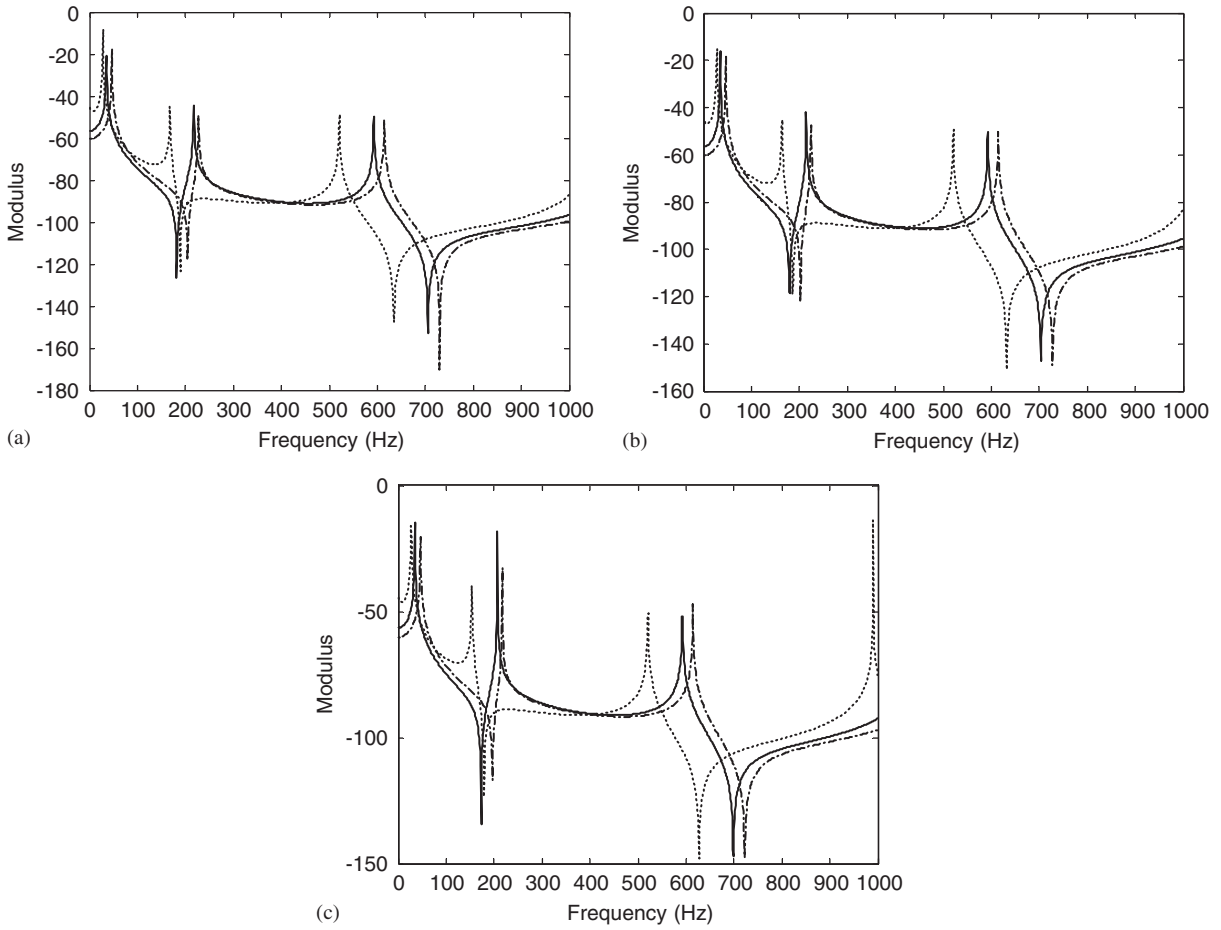

Fig. 8. Frequency responses of the uniform beam with various crack ratios under various axial loadings (—) 0 N, (…) +15 N and (-.-.-) −15 N; (a) without crack, (b) with crack ratio 0.3, (c) with crack ratio 0.5.

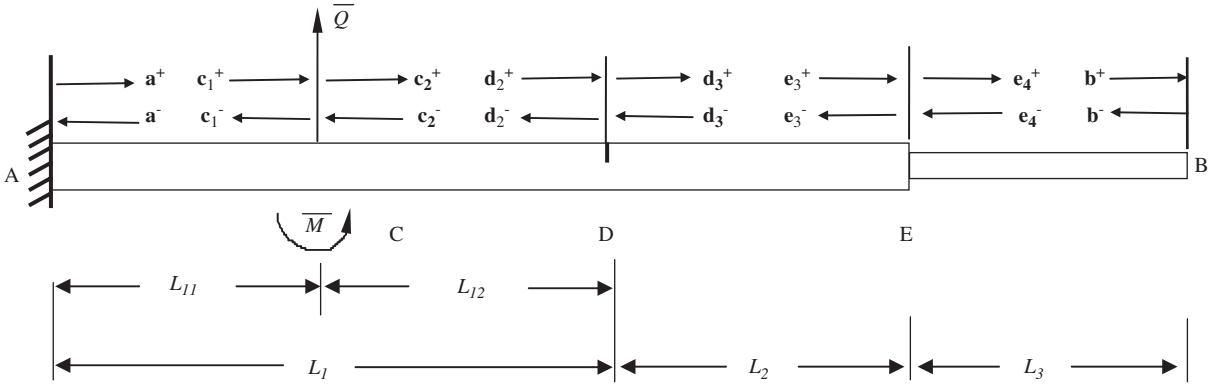

Fig. 9. A cracked stepped cantilever beam with applied force and moment.

(ii) *A stepped beam with a crack*

Fig. 9 shows the cracked stepped beam with a point force and a moment applied at point C. The wave amplitudes at the boundaries, the crack discontinuity and the step change, as well as waves generated by the applied point force and moment, are the same as described in Section 5.1(ii). The propagation relations are redefined as the following:

$$\begin{aligned}
&\mathbf{c}_1^+ = \mathbf{f}(L_{11})\mathbf{a}^+, \quad \mathbf{a}^- = \mathbf{f}(L_{11})\mathbf{c}_1^-, \quad \mathbf{d}_2^+ = \mathbf{f}(L_{12})\mathbf{c}_2^+,\\
&\mathbf{c}_2^- = \mathbf{f}(L_{12})\mathbf{d}_2^-, \quad \mathbf{e}_3^+ = \mathbf{f}(L_2)\mathbf{d}_3^+, \quad \mathbf{d}_3^- = \mathbf{f}(L_2)\mathbf{e}_3^-,\\
&\mathbf{b}^+ = \mathbf{f}(L_3)\mathbf{e}_4^+, \quad \mathbf{e}_4^- = \mathbf{f}(L_3)\mathbf{b}^-,
\end{aligned} \tag{45}$$

where $\mathbf{f}(L_{11})$, $\mathbf{f}(L_{12})$, $\mathbf{f}(L_1)$, $\mathbf{f}(L_2)$ and $\mathbf{f}(L_3)$ are the propagation matrices between AC, CD, DE and EB, respectively.

Writing Eqs. (32), (37) and (45) in matrix form gives

$$\begin{bmatrix}
-\mathbf{I} & \mathbf{r}_a & \mathbf{0} & \mathbf{0} & \mathbf{0} & \mathbf{0} & \mathbf{0} & \mathbf{0} & \mathbf{0} & \mathbf{0} & \mathbf{0} & \mathbf{0} & \mathbf{0} & \mathbf{0} & \mathbf{0} & \mathbf{0}\\
\mathbf{0} & \mathbf{0} & \mathbf{0} & \mathbf{0} & \mathbf{0} & \mathbf{0} & \mathbf{0} & \mathbf{0} & \mathbf{0} & \mathbf{0} & \mathbf{0} & \mathbf{0} & \mathbf{0} & \mathbf{0} & \mathbf{r}_b & -\mathbf{I}\\
\mathbf{0} & \mathbf{0} & -\mathbf{I} & \mathbf{0} & \mathbf{I} & \mathbf{0} & \mathbf{0} & \mathbf{0} & \mathbf{0} & \mathbf{0} & \mathbf{0} & \mathbf{0} & \mathbf{0} & \mathbf{0} & \mathbf{0} & \mathbf{0}\\
\mathbf{0} & \mathbf{0} & \mathbf{0} & -\mathbf{I} & \mathbf{0} & \mathbf{I} & \mathbf{0} & \mathbf{0} & \mathbf{0} & \mathbf{0} & \mathbf{0} & \mathbf{0} & \mathbf{0} & \mathbf{0} & \mathbf{0} & \mathbf{0}\\
\mathbf{0} & \mathbf{0} & \mathbf{0} & \mathbf{0} & \mathbf{0} & \mathbf{0} & \mathbf{r} & -\mathbf{I} & \mathbf{0} & \mathbf{t} & \mathbf{0} & \mathbf{0} & \mathbf{0} & \mathbf{0} & \mathbf{0} & \mathbf{0}\\
\mathbf{0} & \mathbf{0} & \mathbf{0} & \mathbf{0} & \mathbf{0} & \mathbf{0} & \mathbf{t} & \mathbf{0} & -\mathbf{I} & \mathbf{r} & \mathbf{0} & \mathbf{0} & \mathbf{0} & \mathbf{0} & \mathbf{0} & \mathbf{0}\\
\mathbf{0} & \mathbf{0} & \mathbf{0} & \mathbf{0} & \mathbf{0} & \mathbf{0} & \mathbf{0} & \mathbf{0} & \mathbf{0} & \mathbf{0} & \mathbf{r}_{LL} & -\mathbf{I} & \mathbf{0} & \mathbf{t}_{RL} & \mathbf{0} & \mathbf{0}\\
\mathbf{0} & \mathbf{0} & \mathbf{0} & \mathbf{0} & \mathbf{0} & \mathbf{0} & \mathbf{0} & \mathbf{0} & \mathbf{0} & \mathbf{0} & \mathbf{t}_{LR} & \mathbf{0} & -\mathbf{I} & \mathbf{r}_{RR} & \mathbf{0} & \mathbf{0}\\
\mathbf{f}(L_{11}) & \mathbf{0} & -\mathbf{I} & \mathbf{0} & \mathbf{0} & \mathbf{0} & \mathbf{0} & \mathbf{0} & \mathbf{0} & \mathbf{0} & \mathbf{0} & \mathbf{0} & \mathbf{0} & \mathbf{0} & \mathbf{0} & \mathbf{0}\\
\mathbf{0} & -\mathbf{I} & \mathbf{0} & \mathbf{f}(L_{11}) & \mathbf{0} & \mathbf{0} & \mathbf{0} & \mathbf{0} & \mathbf{0} & \mathbf{0} & \mathbf{0} & \mathbf{0} & \mathbf{0} & \mathbf{0} & \mathbf{0} & \mathbf{0}\\
\mathbf{0} & \mathbf{0} & \mathbf{0} & \mathbf{0} & \mathbf{f}(L_{12}) & \mathbf{0} & -\mathbf{I} & \mathbf{0} & \mathbf{0} & \mathbf{0} & \mathbf{0} & \mathbf{0} & \mathbf{0} & \mathbf{0} & \mathbf{0} & \mathbf{0}\\
\mathbf{0} & \mathbf{0} & \mathbf{0} & \mathbf{0} & \mathbf{0} & -\mathbf{I} & \mathbf{0} & \mathbf{f}(L_{12}) & \mathbf{0} & \mathbf{0} & \mathbf{0} & \mathbf{0} & \mathbf{0} & \mathbf{0} & \mathbf{0} & \mathbf{0}\\
\mathbf{0} & \mathbf{0} & \mathbf{0} & \mathbf{0} & \mathbf{0} & \mathbf{0} & \mathbf{0} & \mathbf{0} & \mathbf{f}(L_2) & \mathbf{0} & -\mathbf{I} & \mathbf{0} & \mathbf{0} & \mathbf{0} & \mathbf{0} & \mathbf{0}\\
\mathbf{0} & \mathbf{0} & \mathbf{0} & \mathbf{0} & \mathbf{0} & \mathbf{0} & \mathbf{0} & \mathbf{0} & \mathbf{0} & -\mathbf{I} & \mathbf{0} & \mathbf{f}(L_2) & \mathbf{0} & \mathbf{0} & \mathbf{0} & \mathbf{0}\\
\mathbf{0} & \mathbf{0} & \mathbf{0} & \mathbf{0} & \mathbf{0} & \mathbf{0} & \mathbf{0} & \mathbf{0} & \mathbf{0} & \mathbf{0} & \mathbf{0} & \mathbf{0} & \mathbf{f}(L_3) & \mathbf{0} & -\mathbf{I} & \mathbf{0}\\
\mathbf{0} & \mathbf{0} & \mathbf{0} & \mathbf{0} & \mathbf{0} & \mathbf{0} & \mathbf{0} & \mathbf{0} & \mathbf{0} & \mathbf{0} & \mathbf{0} & \mathbf{0} & \mathbf{0} & -\mathbf{I} & \mathbf{0} & \mathbf{f}(L_3)
\end{bmatrix}
\begin{bmatrix}
\mathbf{a}^+\\ \mathbf{a}^-\\ \mathbf{c}_1^+\\ \mathbf{c}_1^-\\ \mathbf{c}_2^+\\ \mathbf{c}_2^-\\ \mathbf{d}_2^+\\ \mathbf{d}_2^-\\ \mathbf{d}_3^+\\ \mathbf{d}_3^-\\ \mathbf{e}_3^+\\ \mathbf{e}_3^-\\ \mathbf{e}_4^+\\ \mathbf{e}_4^-\\ \mathbf{b}^+\\ \mathbf{b}^-
\end{bmatrix}
=
\begin{bmatrix}
\mathbf{0}\\ \mathbf{0}\\ \mathbf{q}^+\\ \mathbf{q}^-\\ \mathbf{0}\\ \mathbf{0}\\ \mathbf{0}\\ \mathbf{0}\\ \mathbf{0}\\ \mathbf{0}\\ \mathbf{0}\\ \mathbf{0}\\ \mathbf{0}\\ \mathbf{0}\\ \mathbf{0}\\ \mathbf{0}
\end{bmatrix}, \tag{46}$$

from which the magnitudes of the waves can be solved in terms of the external excitations. The deflection of any point along the beam can then be found by following the same procedure as described in Section 5.2(i).

Fig. 10 shows the frequency responses of the stepped beam due to a point force excitation at $0.75L$, with the disturbance force applied at $0.45L$. The natural frequencies agree well with those predicted in Table 4.

From the above analyses, it is seen that, with the availability of the reflection and transmission matrices corresponding to various types of discontinuities, the wave structural vibration analysis of a complex Timoshenko beam is made simple and concise: it involves only a number of matrix operations.

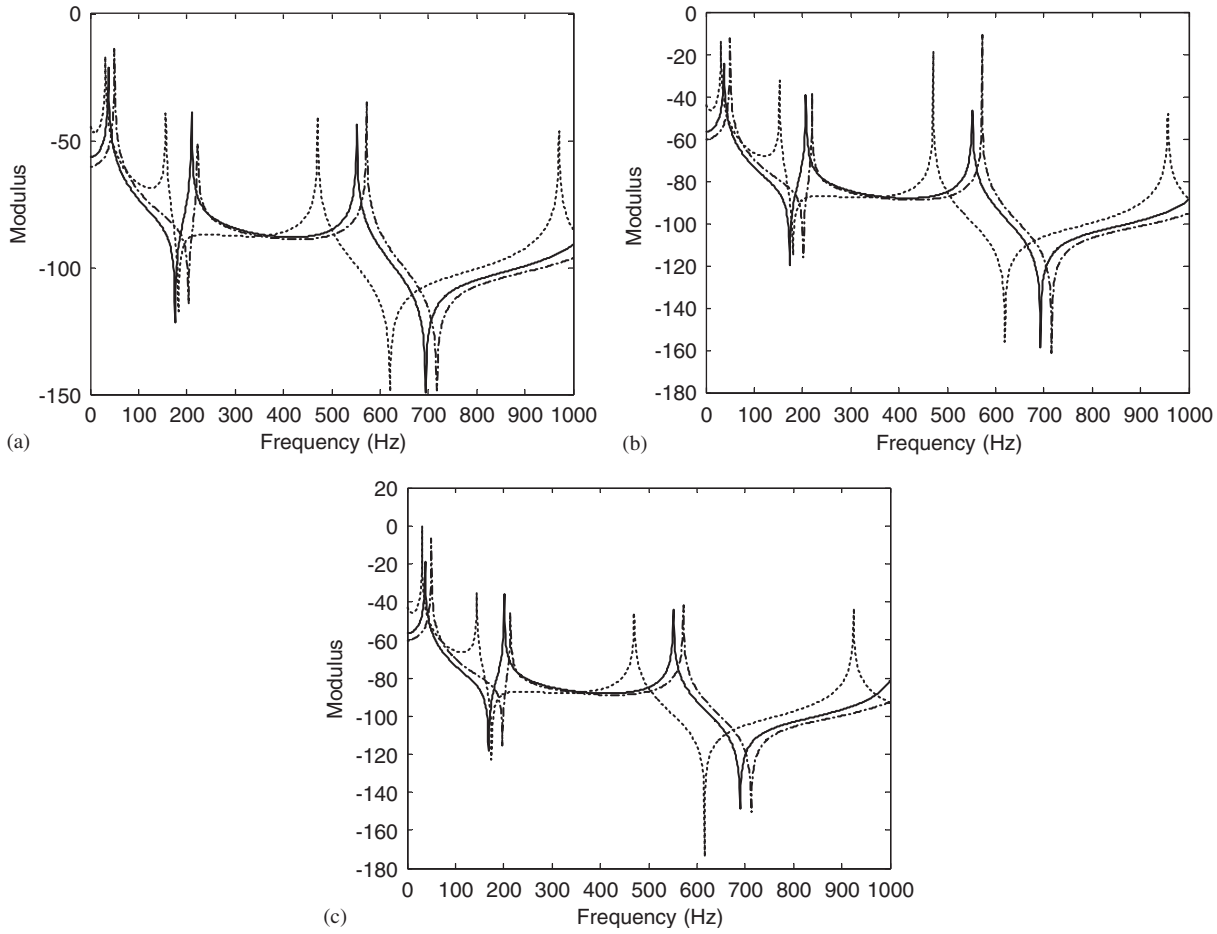

Fig. 10. Frequency responses of the stepped beam with various crack ratio under various axial loading (—) 0 N, (…) +15 N and (-.-.-) −15 N; (a) without crack, (b) with crack ratio 0.3, (c) with crack ratio 0.5.

6. Conclusions

In this paper, wave approach is developed in analyzing both free and forced vibrations of Timoshenko beams under axial loading with various structural discontinuities. Vibration analysis of structures with such complexity is difficulty to perform using the conventional modal approach. Numerical approaches are normally used in finding the solutions. However, with the availability of propagation, reflection and transmission matrices, the exact vibration analysis becomes systematic and concise, as demonstrated through numerical examples. The effects of a crack (including both crack size and crack location), an axial load and a step-structural sectional change on the modes of vibrations are studied in detail.

References

[1] A.D. Dimarogonas, Vibration of cracked structures: a state of the art review, *Engineering Fracture Mechanics* 55 (5) (1996) 831–857.
[2] P. Cawley, R.D. Adams, Structures from measurements of natural frequencies, *Journal of Strain Analysis* 14 (1979) 49–57.
[3] M. Krawczuk, W.M. Ostachowicz, Modeling and vibration analysis of a cantilever composite beam with a transverse open crack, *Journal of Sound and Vibration* 183 (1) (1995) 69–89.
[4] B.P. Nandwana, S.K. Maiti, Detection of the location and size of a crack in stepped cantilever beams based on measurements of natural frequencies, *Journal of Sound and Vibration* 203 (3) (1997) 435–446.
[5] M.H.H. Shen, C. Pierre, Free vibration of beams with a single-edge crack, *Journal of Sound and Vibration* 170 (2) (1994) 237–259.
[6] Y. Narkis, Identification of crack location in vibrating simply supported beams, *Journal of Sound and Vibration* 172 (4) (1994) 549–558.
[7] T.C. Tsai, Y.Z. Wang, Vibration analysis and diagnosis of a cracked shaft, *Journal of Sound and Vibration* 192 (3) (1996) 607–620.
[8] N.T. Khiem, T.V. Lien, The dynamic stiffness matrix method in forced vibration analysis of multiple-cracked beam, *Journal of Sound and Vibration* 254 (3) (2002) 541–555.
[9] K.F. Graff, *Wave Motion in Elastic Solids*, Ohio State University Press, Ohio, 1975.
[10] L. Cremer, M. Heckel, E.E. Ungar, *Structure-Borne Sound*, Springer, Berlin, 1987.
[11] J.F. Doyle, *Wave Propagation in Structures*, Springer, New York, 1989.
[12] B.R. Mace, Wave reflection and transmission in beams, *Journal of Sound and Vibration* 97 (1984) 237–246.
[13] C.A. Tan, B. Kang, Wave reflection and transmission in an axially strained, rotating Timoshenko shaft, *Journal of Sound and Vibration* 213 (3) (1998) 483–510.
[14] N.R. Harland, B.R. Mace, R.W. Jones, Wave propagation, reflection and transmission in tunable fluid-filled beams, *Journal of Sound and Vibration* 241 (5) (2001) 735–754.
[15] C. Mei, B.R. Mace, Wave reflection and transmission in Timoshenko beams and wave analysis of Timoshenko beam structures, *ASME Journal of Vibration and Acoustics* 127 (4) (2005) 382–394.
[16] T.G. Chondros, The continuous crack flexibility model for crack identification, *Fatigue and Fracture of Engineering Materials and Structures* 24 (2001) 643–650.
[17] T.G. Chondros, A.D. Dimarogonas, J. Yao, A continuous cracked beam vibration theory, *Journal of Sound and Vibration* 215 (1) (1998) 17–34.